Neurochem Res (2006) 31:247–257
DOI 10.1007/s11064-005-9013-7

ORIGINAL PAPER

Immunohistochemical Distribution and Subcellular Localization of the Somatostatin Receptor Subtype 1 (sst1) in the Rat Hypothalamus

Thomas Stroh · Philippe Sarret · Gloria S. Tannenbaum · Alain Beaudet

Accepted: 11 October 2005 / Published online: 2 March 2006

Abstract The aim of the present study was to examine the cellular and sub-cellular distribution of the somatostatin (SRIF) receptor subtype sst1 in the rat hypothalamus. Receptors were immunolabeled using an antibody directed against an antigenic sequence in the N-terminus of the receptor. Immunopositive neuronal cell bodies and dendrites were observed throughout the mediobasal hypothalamus, including the medial preoptic area, paraventricular, periventricular, and arcuate nuclei. Immunoreactive axons and axon terminals were also observed in the median eminence, suggesting that sst1 is also located pre-synaptically. Electron microscopic examination of the arcuate nucleus revealed a predominant association of immunoreactive sst1 with perikarya and dendrites. Most immunoreactive receptors were intracellular and localized to tubulovesicular compartments and organelles such as the Golgi apparatus, but 14% were associated with the plasma membrane. Of the latter, 47% were apposed to abbuting afferent axon terminals and 20% localized immediately adjacent to an active synaptic zone. These results demonstrate a widespread distribution of sst1 receptors in rat hypothalamus. They also show that somatodendritic sst1 receptors in the arcuate nucleus are ideally poised to mediate SRIF's modulation of afferent synaptic inputs, including central SRIF effects on growth hormone-releasing hormone neurons documented in this area.

Keywords Somatostatin · sst1 · Growth hormone · Arcuate nucleus · Paraventricular nucleus · Synapse

Special Issue Dedicated to Miklós Palkovits.

T. Stroh (✉) · P. Sarret · A. Beaudet
Department of Neurology & Neurosurgery,
Montreal Neurological Institute, McGill University,
3801, University Street, H3A 2B4, Montréal,
Québec, Canada
E-mail: thomas.stroh@mcgill.ca
Tel.: +(514)-398-1913
Fax: +(514)-398-5871

G. S. Tannenbaum
Departments of Pediatrics and Neurology & Neurosurgery,
Montreal Children's Hospital Research Institute,
McGill University, Montréal, Québec, Canada

P. Sarret
Department of Physiology and Biophysics, Faculty of Medicine,
University of Sherbrooke, Sherbrooke, Québec, Canada

Introduction

The tetradecapeptide somatostatin, also referred to as somatotropin release-inhibiting factor (SRIF) was originally characterized as a hypothalamic factor inhibiting the release of growth hormone (GH) from pituitary somatotropes [1]. It was later shown to be distributed widely throughout the central nervous system and the periphery where it performs a variety of neurotransmitter-like and hormonal functions [for review, 2]. Several lines of evidence suggest that, in addition to acting directly on somatotropes via the median eminence/hypophyseal portal system, SRIF regulates GH release indirectly through central regulation of GH-releasing hormone (GHRH)-containing neurons, although the mechanisms underlying these central effects have not yet been fully defined [for review, 3].

Radioligand binding experiments have demonstrated the presence of SRIF binding sites throughout the neuraxis [for review, 4]. The introduction of smaller cyclic peptide analogs such as octreotide revealed the existence of multiple SRIF receptor subtypes and prompted their classification into two groups, SRIF-1 and SRIF-2, based

on their differential affinity for these analogs [for review, 3]. Molecular cloning studies have since demonstrated the existence of at least five SRIF receptor subtypes, designated sst1–sst5 [for review, 5–7]. All of these are G protein-coupled and are linked to a variety of intracellular messenger systems such as adenylate cyclase, various ion channels, extracellular signal-regulated kinases and protein phosphatases [for review, 6].

The cloning of sst1–5 receptor subtypes opened the lane towards the development of receptor subtype-specific mRNA probes and anti-peptide antibodies. The distribution of mRNAs for all SRIF receptor subtypes has been extensively studied using in situ hybridization histochemistry and RNase protection assay, revealing the presence of all subtypes in the brain, albeit at varying extents [8–12]. Thus, sst1–sst3 were found to be expressed in a considerably more widespread manner than sst4 and sst5 [12]. In the hypothalamus, in situ hybridization studies suggest that sst1 and sst2 are the most abundant SRIF receptor subtypes [13]. Furthermore, both sst1 and sst2 mRNAs were found to be expressed by GHRH mRNA-containing neurons in the ventromedial aspect of the arcuate nucleus [14]. In agreement with these findings, both receptor subtypes were shown to be involved in the hypothalamic regulation of GH secretion [15–18].

The distribution of SRIF receptor proteins, as revealed by immunohistochemical studies, largely conforms to that of their corresponding mRNAs [8–13, 19–28], with the exception of sst1 for which major discrepancies exist in the literature. Thus, whereas a study employing an anti-peptide antibody directed against the N-terminal domain of human sst1 found this receptor to be widely distributed throughout the rat brain [23], in a pattern reminiscent of that revealed by in situ hybridization [8–11, 13], another study using an antibody raised against a C-terminal peptide of human sst1, found it to be restricted to the parvocellular periventricular system of the rat hypothalamus including axonal terminals in the outer zone of the median eminence [22].

In the present study, we sought to re-evaluate the distribution of sst1 receptor proteins in rat brain with special emphasis on the hypothalamus, as well as to characterize their subcellular localization within hypothalamic neurons. To this end, we raised several antisera against different peptides from the deduced amino acid sequence of rat sst1. One antiserum directed against an N-terminal peptide and another anti-C-terminal serum were specific and sensitive for use for both light and electron microscopic immunohistochemistry.

Experimental procedures

All animal-related procedures were approved by the McGill University Animal Care Committee and carried out according to the regulations of the Canadian Council on Animal Care.

Primary antibody for sst1 immunodetection

Rabbit anti-sst1 peptide antisera were generated using synthetic peptides (PGGCGEGVCSRGPGS and PENLESGGVFRNGTC, respectively) corresponding to the 18–32 predicted amino acid sequence in the N-terminus and amino acids 370–384 in the C-terminus of the rat receptor [29, 30], and showing no homology with other known SRIF receptor subtypes. The peptides were conjugated via maleimide to ovalbumin (Affinity BioReagents, ABR, Golden, CO, USA). The conjugates were used to immunize two rabbits each. The initial immunization was followed by five additional booster injections. Serum samples were analysed separately for reactivity by Western blotting and immunohistochemistry. In each pair of antisera (N-terminal and C-terminal, respectively) one serum was found to be more sensitive than the other for immunohistochemistry. Those two sera were employed in the present study.

Culture and transfection of COS-7 cells

COS-7 cells were maintained in Dulbecco's modified Eagle's medium with high glucose supplemented with 5% fetal bovine serum in the presence of 100 U/ml penicillin/streptomycin (GibcoBRL, Life Technologies, Burlington, ON, Canada). Cells were grown at 37°C in a humidified atmosphere with 5% CO_2 and plated in 100 mm Petri dishes at a density of 10^6 cells/dish. On the following day, semiconfluent cells were transiently transfected with the rat sst1 receptor cDNA by the DEAE-dextran/chloroquine method, as described previously [31]. Cells were collected 48–72 h after the beginning of the transfection and processed for immunoprecipitation or immunocytochemistry as described below.

Immunoblotting analysis

For Western blot analysis, transfected and non-transfected COS-7 cells were grown in 100 mm culture dishes, harvested with 1 ml trypsin-EDTA (Life Sciences, Burlington, ON, Canada), centrifuged briefly, resuspended in 1 ml of 50 mM Tris–HCl (pH 7.0) and 4 mM EDTA with protease inhibitors (CompleteTM Protease inhibitors tablets, Roche Molecular Biochemicals, Laval, QC, Canada), homogenized by sonication, and centrifuged at 4°C for 30 min at 13,500 rpm. The pellets were then resuspended in 50 mM Tris–HCl (pH 7.0) and 0.2 mM EDTA with protease inhibitors, by vortexing and brief sonication. Protein concentration of the samples was determined using the Bradford procedure. The membranes were subsequently

denatured using Laemmli sample buffer and 20 μg of protein/lane were loaded onto 8% Tris–Glycine precast gels (Invitrogen, Burlington, ON, Canada). Resolved proteins were transferred to nitrocellulose membranes (BioRad laboratories, Mississauga, ON, Canada). Non-specific sites were blocked by 0.1% Tween 20 and 10% milk powder (Carnation, Don Mills, ON, Canada) in phosphate-buffered saline (PBS; pH 7.4) overnight at 4°C. Nitrocellulose membranes were then immunoblotted overnight at 4°C with anti-sst1 antisera diluted 1:1000 in PBS with 1% BSA and 1% ovalbumin. After washing with PBS–Tween, blots were incubated for 1 h at room temperature (RT) with HRP-conjugated goat anti-rabbit secondary antibodies (1:4000; Amersham Pharmacia Biotech, Baie d'Urfé, QC, Canada) in PBS with 5% milk powder and proteins were visualized by means of an enhanced chemiluminescent detection system (Perkin Elmer, Life Sciences, Boston, MA).

Immunocytochemistry on COS-7 cells

Sst1-transfected and non-transfected COS-7 cells, plated on poly-L-lysine-coated glass coverslips, were fixed for 20 min with 4% paraformaldehyde (PFA; Polysciences, Warington, PA, USA) in 0.1 M phosphate buffer (PB), pH 7.4, rinsed with 0.1 M Trisma base-buffered saline (TBS), pH 7.4, and pre-incubated for 30 min at RT with a blocking solution consisting of 5% normal goat serum (NGS), 2% BSA and 0.1% Triton X-100 (BDH Inc., Toronto, ON, CAN) in 0.1 M TBS. Cells were then incubated overnight at 4°C with the anti-sst1 peptide antisera (1:1000), in the absence of antiserum, or with antisera pre-adsorbed with the antigenic peptide diluted 1:1000 in 0.1 M TBS, pH 7.4, containing 1% NGS and 0.05% Triton X-100. After washing with TBS, cells were incubated for 1 h at RT with Alexa-488-conjugated goat anti-rabbit (1:800; Molecular Probes, Eugene, OR, USA), washed twice in TBS and mounted on glass slides with Aquamount.

Labeled cells were analysed by confocal microscopy using a Leica confocal laser scanning microscope (CLSM) configured with a Leica Fluovert FS inverted fluorescence microscope and equipped with an argon/krypton laser with an output power of 2–50 mV and a VME bus MC 68020/68881 computer system running the Leica CLSM software package (Leica, Dollard des Ormeaux, QC, Canada). Alexa-488 immunofluorescence was detected by excitation at 488 nm. Images were acquired as single optical sections taken through the middle of the cells and averaged over 16 scans/frame. They were transferred to an IBM-compatible personal computer using CaptureIt Bitman version 1.0.59 image capture and transfer software (Meridian Scientific Services Inc., Carp, ON, Canada) and archived on CD-ROM. Processing was carried out using Adobe Photoshop 6.0 (Adobe Systems Inc., San Jose, CA) and Powerpoint software (Microsoft, Redmond, WA). Identical parameters were used to acquire the images for cells immunolabelled in the presence or absence of sst1 antiserum, for non-transfected cells, and cells incubated with pre-adsorbed antiserum.

Immunohistochemistry

Light microscopy

Adult male Sprague-Dawley rats (200–250 g; $n = 4$) were purchased from Charles River Canada (St. Constant, QC, Canada) and housed on a 12 h light, 12 h dark cycle (lights on, 0600–1800 h) in a temperature- (22 ± 1°C) and humidity-controlled room. Rat chow (Ralston Purina Co., St. Louis, MO) and tap water were available ad libitum. On the test day, the rats were anesthetized with sodium pentobarbital (65 mg/kg i.p.) and perfused transaortically with a freshly prepared solution of 4% PFA and 0.2% picric acid in 0.1 M PB pH 7.4 (modified Zamboni fixative). Brains were rapidly removed, cryoprotected overnight at 4°C in 0.1 M PB containing 30% sucrose, and frozen for 1 min in isopentane at −40°C.

Coronal sections (30 μm-thick) were cut on a freezing microtome throughout the rostro-caudal extent of the hypothalamus from the preoptic area to the mammillary region and collected in 0.1 M PB. Immunohistochemistry was performed according to the avidin biotinylated-HRP complex (ABC) method using an *Elite* ABC kit (Vector Laboratories, Burlingame, CA) as previously described [32]. Briefly, free-floating sections were washed twice with 0.1 M Trisma base-buffered Saline (TBS), pH 7.4 and pre-treated for 30 min with 3% hydrogen peroxide in 0.1 M TBS to quench endogenous peroxidase. Serial sections were then incubated for 30 min at RT in a blocking solution containing 3% normal goat serum (NGS) in TBS and overnight at 4°C with the respective sst1 antiserum (N-terminal or C-terminal-directed) diluted 1:500 in TBS containing 0.05% Triton X-100 and 0.5% NGS. Control sections were either incubated with antiserum pre-adsorbed with 1 mg/ml antigenic peptide or in the absence of primary antibody. The following day, sections were rinsed in TBS (2×10 min) and incubated for 45 min at RT in biotylinated goat anti-rabbit immunoglobulin diluted 1:400 in TBS (Vector Laboratories), followed by 45 min in ABC solution (prepared according to the manufacturer's instructions). Visualization of bound peroxidase was achieved by reaction for 6 min in a solution of 0.1 M Tris–HCl (TB; pH 7.4) containing 0.05% 3-3′-diaminobenzidine (DAB, Sigma-Aldrich, Oakville, ON, Canada), 0.04% nickel chloride and 0.0075% H_2O_2. The reaction was stopped by several washes with 0.1 M TBS.

Sections were mounted on chrome alum/gelatin-coated slides, dehydrated in graded ethanols, defatted in xylene and covered with Permount (Fisher Scientific, Montreal, QC, Canada). Labelled structures were examined under bright-field illumination under a Leitz Aristoplan microscope (Leica, Dollard des Ormeaux, QC, Canada). Digital images were acquired with a Pulnix TMC−1000CL camera using VisionGauge software (VISIONx INC., Montreal, QC, Canada) and the final composites were processed using Adobe Photoshop 6.0 (Adobe Systems Inc., San Jose, CA) and Powerpoint software (Microsoft, Redmond, WA) on an IBM-compatible computer. Hypothalamic nuclei were identified according to the nomenclature of Paxinos and Watson's atlas.

Electron microscopy

Sections were processed for electron microscopy using a pre-embedding procedure as described previously [33–35]. Adult male Sprague–Dawley rats (250–325 g; $n = 5$) were anesthetized with sodium pentobarbital (35 mg/kg, i.v.) and perfused trans-aortically with 50 ml of heparinized saline (10 U/ml in 0.9% NaCl) followed by 50 ml of a mixture of 3.75% acrolein and 2% PFA in 0.1 M PB, and then by 300 ml of 2% PFA in 0.1 M PB, pH 7.4. Brains were rapidly removed from the skull and post-fixed for 30 min in the 2% PFA solution. Sections (50 μm-thick) of the hypothalamus were cut on a vibratome, collected in 0.1 M PB and incubated in a solution of 1% sodium borohydride in PB for 30 min to neutralize free aldehyde groups. Following extensive rinsing with PB, they were cryoprotected for 30 min by immersion in a mixture of 25% sucrose and 3% glycerol in 0.1 M PB, rapidly frozen in isopentane at −60°C, briefly transferred to liquid nitrogen, and finally thawed in PB at room temperature. Thawed sections were pre-incubated for 30 min in 0.1 M TBS (pH 7.4) containing 3% NGS and then incubated overnight at 4°C in rabbit sst1 N-terminal antiserum diluted 1:200 in TBS containing 0.5% NGS. After rinsing in 0.01 M PBS, sections were incubated for 2 h at RT in a 1:50 dilution of ultrasmall colloidal gold-conjugated goat anti-rabbit immunoglobulin (Aurion, Amsterdam, Netherlands) diluted in PBS containing 0.2% gelatin and 0.8% BSA. After several washes in PBS, sections were fixed for 10 min in 2% glutaraldehyde in PBS, washed in PBS, and rinsed twice in 0.2 M citrate buffer, pH 7.4. Immunogold particles were amplified through silver intensification by incubating the sections for 8 min with IntenSE M silver solution (Amersham Biosciences, Piscataway, NJ). The reaction was stopped by washing in citrate buffer and 0.1 M PB pH 7.4. Subsequent to post-fixation in 2% osmium tetroxide in 0.1 M PB for 40 min, the sections were dehydrated in graded ethanols and infiltrated with propylene oxide followed by Epon 812 (1:1 then 1:3, respectively). The mixture was replaced by 100% Epon 812 and incubated overnight at 4°C followed by placement between two sheets of acetate at 60°C for 24 h for flat-embedding. Ultrathin sections (80-nm thick) were collected from the arcuate nucleus (between the retrochiasmatic area anteriorly and the mammillary bodies posteriorly), counterstained with uranyl acetate/lead nitrate and examined with a JEOL 100CX transmission electron microscope.

For analysis of the subcellular distribution of silver-enhanced gold particles, sections (approximately 100 sections in total, collected from 2 blocks per animal) were randomly scanned and each field exhibiting gold particles was photographed at an original magnification of 5–10,000×. Additional sections from tissue incubated in the absence of primary antibodies were also scanned in each animal to assess non-specific background labelling. Negatives from electron microscopic photomicrographs were scanned at 1200 dpi resolution on an AGFA Duoscan T1200 scanner (AGFA Canada, Pointe Claire, QC, Canada). The digitized negatives were processed using Adobe Photoshop 6.0 (Adobe Systems Inc., San Jose, CA) and MS Powerpoint software (Redmond, WA) on an IBM-compatible computer. Gold particles were then classified according to the type of tissue component, perikarya or dendrites, with which they were associated. Dendrite- and cell body-associated grains were further classified as intracellular or membrane-associated. Membrane-associated grains were also characterized as facing (or not) abutting afferent axon terminals. Of those, particles directly overlying or located immediately adjacent to an active zone were differentiated from those facing an apposed terminal devoid of synaptic specialization. Calculations were performed using MS Excel 2000 (Redmond, WA) and Origin release 6.1 (OriginLab Corp., Northampton, MA). Data were expressed as percentages ± standard error.

Results

Characterization of anti-sst1 sera

To characterize the specificity of the sst1 antisera, Western blotting was performed on membranes prepared from COS-7 cells transfected with rat sst1 cDNA. No signal was obtained in Western blotting using the C-terminal serum, whereas the N-terminal antiserum recognized bands at approximately 60 kDa (Fig. 1a), corresponding to the expected size of the receptor, as deduced from its cDNA sequence [36]. In addition, a major band was detected migrating at approximately twice that molecular weight (Fig. 1a).

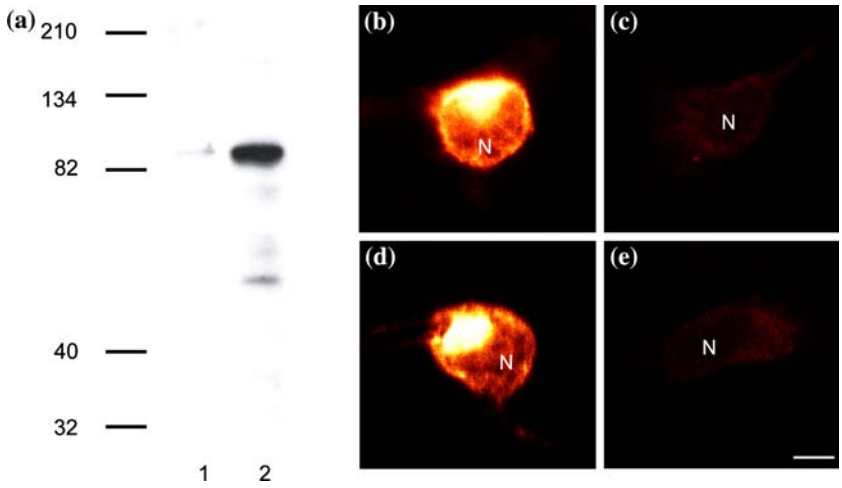

Fig. 1 Characterization of sst1 antisera. **(a)** Membranes prepared from wild-type COS-7 cells (lane 1) and from COS-7 cells transfected with cDNA encoding the rat sst1 receptor (lane 2) were resolved in SDS-PAGE, blotted and exposed to the N-terminally directed sst1-antiserum. Protein bands are evident at approximately 60 kDa, corresponding to the size of sst1, and at approximately twice that size. The latter band presumably corresponds to multimeric form(s) of sst1. **(b, d)** In rat sst1-transfected COS-7 cells, both N-terminally **(b)** and C-terminally **(d)** directed antisera produce intense sst1-like immunolabelling throughout the cell body except for the nucleus (N). **(c, e)** This staining is completely absent from non-transfected wild type COS-7 cells. Scale bar = 10 μm

To demonstrate the applicability of the antisera to immunocytochemical detection of sst1 in aldehyde-fixed material, transfected cells were incubated with either one of the two antisera and examined under a confocal microscope. Both N- and C-terminal antisera produced intense intracellular staining, sparing the nucleus (Fig. 1b, d). In addition, the cell periphery was outlined by a slim margin of immunofluorescence, suggestive of cell surface staining (Fig. 1b, d). No staining was observed in non-transfected COS-7 cells incubated with either antiserum (Fig. 1c, e) or after omission of primary antibodies or pre-adsorption of the sera with an excess of antigenic peptide (not shown).

Regional and cellular distribution of sst1 in the hypothalamus

N- and C-terminal antisera produced the same pattern of immunolabelling in Zamboni-fixed rat brain sections. This staining was abolished in sections incubated in the absence of primary antiserum (not shown) or with antiserum pre-adsorbed with an excess of antigenic peptide (compare Fig.2a, b; see also Fig. 3d). The pattern of sst1 immunolabelling corresponded closely to the reported distribution of sst1 mRNA by in situ hybridization histochemistry and RNase protection assay [8–13] as illustrated here for the arcuate nucleus (Fig. 3a, b). Thus, the neocortex, hippocampus and hypothalamus all showed intense sst1-like immunolabelling, whereas the thalamus exhibited only extremely low levels of staining (data not shown). However, the C-terminal antiserum was clearly less sensitive than its N-terminal counterpart. Therefore, our analysis of the distribution of sst1 in the hypothalamus was carried out using the N-terminal serum.

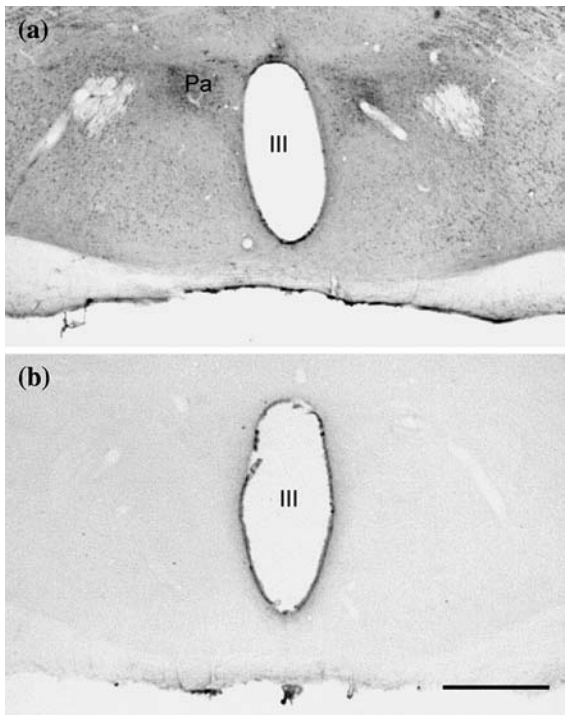

Fig. 2 Specificity of sst1-like immunolabelling in rat hypothalamus. Coronal sections of the mediobasal hypothalamus (level of the anterior paraventricular nucleus; Pa) immunostained with N-terminal sst1 antiserum in the presence **(b)** or the absence **(a)** of pre-adsorbed antiserum (1 mg/ml antigenic peptide). Note the presence of widespread sst1-like immunoreactivity, most conspicuously in the Pa, in **(a)** and the complete abolition of sst1 immunostaining in **(b)**. III = third ventricle. Scale bar = 1,100 μm

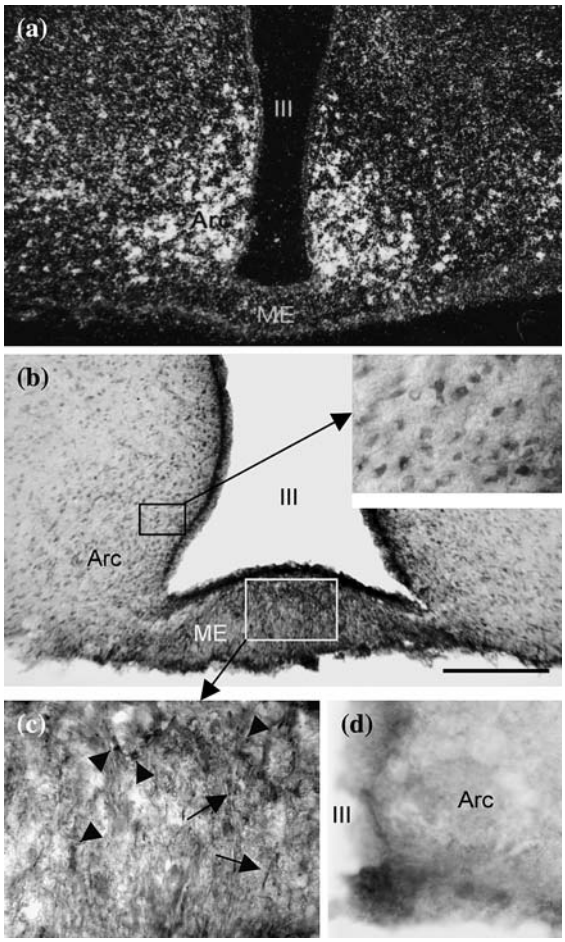

Fig. 3 Comparison of the distributions of sst1 mRNA (**a**; reprinted from Beaudet et al. (1995) with permission) and sst1-like immunoreactivity **(b)** in the rat hypothalamus (level of the arcuate nucleus; Arc). **(a)** Sst1 mRNA-expressing cells are visualized by in situ hybridization using liquid emulsion autoradiography. A strong signal is apparent over a subpopulation of arcuate neurons, as well as lateral to the arcuate proper. **(b)** The same areas display numerous sst1-like immunoreactive nerve cell bodies in sections stained with our N-terminally directed antiserum. The median eminence (ME) also exhibits prominent fiber staining. **(c)** At high magnification, immunoreactive processes (arrows) as well as puncta typical of labelled axonal varicosities (arrowheads) are apparent in the ME. **(d)** Pre-adsorption of the antiserum abolishes immunostaining in the Arc. III = third ventricle. Scale bar: **a** = 500 μm; **b** = 250 μm; **c**, **d**, insert in **(b)** = 100 μm

Throughout the hypothalamus, sst1-like immunoreactivity was predominantly associated with nerve cell bodies and dendrites (e.g., Figs. 3b, 4). No beaded fibers typical of immunolabelled varicose axons were evident in any of the hypothalamic nuclei examined. However, within the median eminence, immunoreactive fibers as well as puncta reminiscent of axonal varicosities were clearly discernable (Fig. 3b, c), suggesting that sst1-like immunoreactivity may also be associated with axons. No obvious sst1 immunostaining was observed over glial cells.

Nuclei in all sub-regions of the hypothalamus displayed sst1-like immunoreactivity. However, sst1-like immunostaining was mainly concentrated in the mediobasal hypothalamus, adjacent to the third ventricle (Figs. 3, 4). The medial preoptic area (Fig. 4b) and anterior periventricular nucleus exhibited moderately intense sst1-like immunoreactive nerve cell bodies. The paraventricular nucleus displayed large numbers of immunopositive neuronal cell bodies and dendrite-like immunoreactive processes throughout its rostro-caudal extent (Figs. 2a, 4b, c). Anteriorly, strongly stained magnocellular neurons were evident in the lateral aspect of the nucleus. Medially and ventrally to the magnocellular areas, less densely clustered neurons were stained in the parvocellular portions of the nucleus (Fig. 4a, b, d). Scattered immunoreactive perikarya were seen throughout the periventricular nucleus (Fig. 4a, b). In the arcuate nucleus, moderately to strongly sst1-like immunopositive cells were concentrated in the ventromedial aspect of the nucleus (Fig. 3b). In addition, some dendrites were faintly labelled (Fig. 3b, insert). This labelling was abolished by pre-adsorption of the antibody with its immunogenic peptide (Fig. 3d). Numerous weakly- to moderately-stained nerve cell bodies were also evident in the ventro-medial nucleus. In the posterior hypothalamus, the pre-mammillary and tubero-mammillary nuclei harboured moderately to strongly stained neurons, whereas the medial mammillary nucleus was only weakly stained at this level. However, in the mammillary region proper, the medial mammillary nucleus displayed moderate labelling, whereas both the lateral and the supramammillary nucleus harboured strongly stained perikarya.

Subcellular distribution of sst1

At the electron microscopic level, silver intensified gold particles indicative of sst1 immunoreactive receptors were primarily found over both perikarya and dendrites of arcuate neurons (Fig. 5). Axonal and terminal profiles were sparsely labelled. No immunostaining was observed over glial profiles (Fig. 5a). In both nerve cell bodies and dendrites, sst1-like immunoreactivity was predominantly intracellular (86 ± 2% of gold particles; $n = 5$ animals, 1,353 particles). These intracellular grains were found in association with the Golgi apparatus and the endoplasmic reticulum as well as with a variety of vesiculotubular organelles including endosomes (Fig. 5b, c).

Cell surface-bound silver-intensified gold particles accounted for 14 ± 2% of the total number of grains ($n = 5$ animals, 1,353 silver particles). Of these cell surface receptors, 47 ± 7% overlaid segments of the membrane adjacent to afferent axon terminals (Fig. 5d). Not all of these abutting terminals displayed a synaptic specialization in the plane of section. However, when they did,

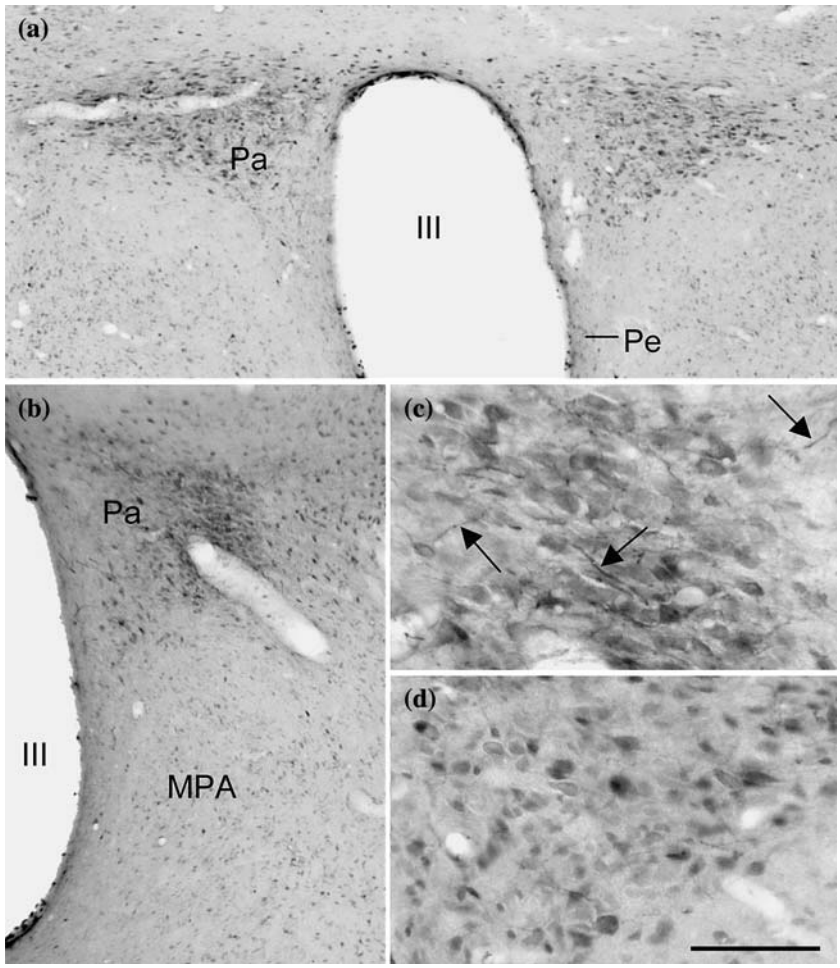

Fig. 4 Distribution of sst1-like immunoreactivity in the paraventricular nucleus of the hypothalamus. **(a, b)** Intensely sst1-like immunostained perikarya are evident in the dorso-lateral segment of the paraventricular nucleus (Pa). Less densely packed immunopostive neurons are evident in medio-ventral subnuclei. Further medio-ventrally, the medial preoptic area (MPA) exhibits lightly labelled neurons. **(c, d)** High magnification of magnocellular **(c)** and parvocellular **(d)** paraventricular nerve cell bodies and dendritic processes (**c**, arrows). Pe = periventricular nucleus; III = third ventricle. Scale bar: **a**, **b** = 500 μm; **c**, **d** = 100 μm

immunolabelled receptors were characteristically located immediately lateral to the active synaptic zone, outside the synaptic gap (Fig. 5e). In fact, 20 ± 3% of membrane-associated receptors occupied such perisynaptic localization. A few gold particles directly overlaid the post-synaptic density itself, although the latter localization was relatively rare.

Discussion

The present study confirms that sst1 receptors are distributed throughout the hypothalamus of adult rats and provides the first description of this receptor's subcellular compartmentalization in the CNS.

Sst1-immunoreactive receptors were visualized using one of two antisera, directed against the N-terminus and the C-terminus of the receptor, respectively. The antigenic peptide sequences chosen were unique to the sst1 receptor subtype and differed from the sequences used to generate previously used sst1 antisera [23, 36, 37]. The specificity of the antisera was first established in immunoblots of sst1-transfected COS-7 cell membranes. The N-terminal antiserum recognized bands of approximately 60 kDa, corresponding to the size of the glycosylated receptor protein [36], as well as higher molecular weight species, suggesting that sst1 may form dimeric or oligomeric complexes. None of these bands were present in non-transfected cells indicating that the serum specifically recognized the sst1 receptor protein. No signal was obtained in Western blotting using the C-terminal serum.

To establish the applicability of these antisera to sst1 immunocytochemistry and to further corroborate their specificity for sst1, immunocytochemical staining was carried out in COS-7 cells transiently transfected with cDNA encoding the rat sst1 receptor protein. In these experiments, both antisera strongly stained sst1-transfected cells, revealing sst1-like immunoreactive material in the periphery of the cells and in juxtanuclear compartments, presumably the Golgi apparatus and/or the Trans-Golgi-Network. The pattern of cellular sst1 distribution observed here in COS-7 cells was reminiscent of the distribution previously described for endocrine cells expressing an epitope-tagged sst1 receptor [38]. Incubation of non-transfected cells with the antisera, or of transfected cells with pre-adsorbed serum or with dilution buffer lacking

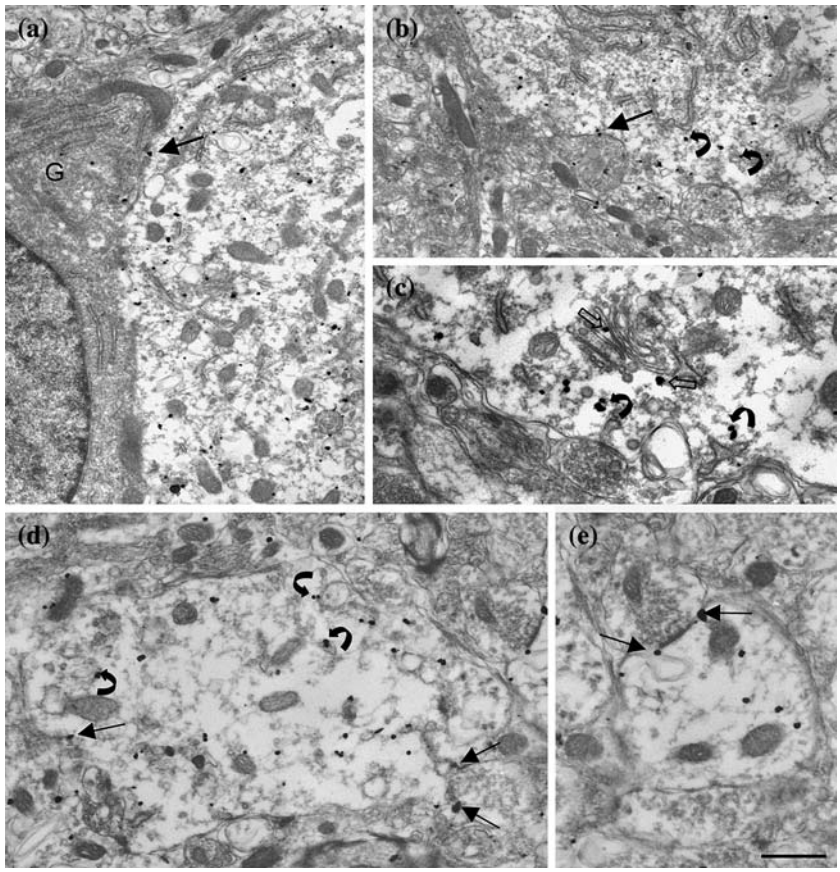

Fig. 5 Ultrastructural distribution of sst1-like immunoreactivity in the rat arcuate nucleus. **(a–c)** Labelled nerve cell bodies. Note that the bulk of silver-intensified gold particles is intracellular and that only a few particles directly overlie the plasma membrane (arrows). Adjacent glial cells (G) are devoid of labelling. Intracellular grains are associated with various tubulo-vesicular organelles such as endocytic vesicles (curved arrows) and the Golgi apparatus (open arrow). **(d, e)** Labelled dendrites. As in cell bodies, labelling in dendrites is mostly intracellular and associated with vesicular organelles (curved arrows). Of the few silver grains associated with the membrane, many are located opposite abutting axon terminals, often immediately adjacent to an active zone (arrows). Scale bar: **a**, **b** = 1.0 μm; **d** = 0.65 μm; **c**, **e** = 0.5 μm

antiserum, completely abolished staining indicating that the antisera were specific for sst1.

Sst1-like immunolabelling detected here in sections of rat brain was also specific, in that it was totally abolished in sections incubated in the absence of primary antibodies or with antiserum pre-adsorbed with an excess of antigenic peptide. Accordingly, the distribution of sst1-immunoreactive nerve cell bodies closely conformed to that of sst1 mRNA revealed by in situ hybridization [8–11, 13], with two exceptions: the suprachiasmatic nucleus, which was immunonegative here but had been reported to express sst1 mRNA [8, 13, 15; but see also 10], and the mammillary nuclei which, conversely, were strongly immunopositive here but had been reported to show only weak mRNA expression [10, 13; but see also 8].

The distribution of sst1 immunoreactivity demonstrated here in the rat hypothalamus also corresponded very closely to the distribution of sst1 revealed in a previous study using an antibody raised against a human N-terminal sequence [23]. However, it was considerably more widespread than in Helboe's study [22], based on immunostaining with an antibody directed against the C-terminus of human sst1. Interestingly, the only regions found to be sst1-positive in this earlier report, namely the periventricular and arcuate nuclei and the median eminence, were among the most strongly labelled ones both in the present study and in earlier in situ hybridization work [13]. These areas also happen to exhibit among the highest levels of SRIF immunoreactivity in the brain [39, 40] and have been documented to play a major role in the regulation of GH secretion [for review, 3, 41].

Indeed, SRIF has been shown to interact with GHRH neurons in the hypothalamic arcuate nucleus to modulate GH release from the pituitary [for review, 3, 41]. In situ hybridization studies have demonstrated high concentrations of sst1 mRNA in the arcuate nucleus [8–11, 13–15, 17], and specifically within GHRH-expressing neurons [14], implying a functional role for the sst1 receptor subtype in modulating GHRH neuronal activity and, presumably, GHRH release into hypophyseal portal blood. Moreover, oligonucleotides designed to knock down sst1 specifically inhibited the modulation of excitability of hypothalamic GHRH neurons through sst1 in vitro and diminished the amplitude of ultradian GH pulses in male rats in vivo [18]. The present results confirm that the receptor protein is present in a large number of cells in the arcuate nucleus and support the notion of sst1 as a major player in the hypothalamic regulation of GH release. In addition, the localization of sst1 receptors on axonal terminals in the median eminence demonstrated here and by

Helboe et al. [22] suggests an involvement of sst1 in the mediation of potential pre-synaptic SRIF effects on the release of hypothalamic releasing and release-inhibiting hormones.

Our electron microscopic observations provide the first description of the subcellular compartmentalization of sst1 in the adult rat brain. Within the arcuate nucleus, which was the only structure examined here, sst1-immunoreactive receptors were predominantly associated with neuronal perikarya and dendrites. Most of these receptors were intracellular, and associated with membranous organelles such as the endoplasmic reticulum, the Golgi apparatus and various kinds of presumptive transport vesicles. This pattern of sub-cellular distribution is reminiscent of that observed for the sst2A receptor subtype in areas receiving a dense somatostatinergic innervation [33]. By contrast, in areas receiving a sparse SRIF innervation, most of sst2A receptors were associated with the plasma membrane [33], which led to the hypothesis that in areas of dense SRIF innervation, cell surface sst2A receptors are chronically down-regulated through binding and internalization of endogenously released SRIF [34, 42]. Since the arcuate nucleus receives substantial somatostatinergic projections from the periventricular nucleus, the subcellular pattern of sst1 distribution observed here, may similarly be due to receptor internalization. The frequent labelling of vesicles resembling endocytic organelles supports this notion.

Of the 14% of immunoreactive receptors associated with the plasma membrane, almost 50% were apposed to afferent synaptic terminals. Moreover, 20% of membrane-associated receptors were located immediately laterally to an active synaptic zone in a perisynaptic position or, more rarely, over the post-synaptic differentiation. This predominance of membrane-associated grains in the vicinity of synapses, raises the question whether more sst1 receptors are, in fact, associated with post-synaptic densities but are unlabelled due to steric hindrance interfering with antibody access to antigens embedded in the protein mesh of the density itself. This appears unlikely, however, since using the same pre-embedding immunogold technique, as employed here, Wang et al. [43] were able to localize the NMDA receptor subunit 1 to post-synaptic densities in a subset of asymmetric synapses in the neostriatum. Moreover, the presence, albeit infrequent, of subsynaptic sst1 receptors in our material suggests that the antibodies have access to receptors embedded in the post-synaptic density. Therefore, the predominant perisynaptic localization of gold particles observed here likely represents a preferential localization of membrane-associated sst1 receptors.

Perisynaptic localization is unusual for neuropeptide receptors. Membrane-bound sst2A receptors, for instance, show no preferential localization for synapses or their vicinity [33]. However, other G protein-coupled receptors have been localized next to synapses. Thus, the metabotropic glutamate receptors mGluR1 and mGluR5 were shown to form a ring around asymmetric synapses in the hippocampus [44, 45]. This perisynaptic localization of the metabotropic glutamate receptors appears to reflect their purported role in modulating synaptic efficacy at glutamatergic synapses, thus promoting synaptic plasticity [for review, 46]. Therefore, the high proportion of perisynaptic cell surface sst1 receptors observed here could imply that this receptor subtype mediates modulatory effects of SRIF on afferent synaptic transmission.

Taken together, our results demonstrate the presence of the sst1 receptor protein in numerous hypothalamic nuclei, including those involved in the mediation of SRIF–GHRH interactions for the regulation of GH release. They also show that in the arcuate nucleus, this receptor subtype is located predominantly intracellularly and that a significant proportion is localized at the periphery of active synaptic zones, indicating that sst1 may mediate SRIF effects on hypothalamic neurons by modulating synaptic inputs to these cells.

Acknowledgements The authors wish to extend their thanks to Mariette Lavallée, Clélia Tommi, Qingyi Chen, and Marwan Samia for expert technical assistance. Ms. Amélie Perron was helpful in performing the immunoblots. This study was supported by Grant MOP−7366 to A.B. and Grant MOP−64328 to G.S.T. from the Canadian Institutes of Health Research; P.S. was recipient of a post-doctoral fellowship by the Fonds de la Recherche en Santé du Québec; G.S.T. holds a career investigator award from the Fonds de la Recherche en Santé du Québec.

References

1. Brazeau P, Vale W, Burgus R, Ling N, Butcher M, Rivier J, Guillemin R (1973) Hypothalamic polypeptide that inhibits the secretion of immunoreactive pituitary growth hormone. Science 179:77–79
2. Epelbaum J, Dournaud P, Fodor M, Viollet C (1994) The neurobiology of somatostatin. Crit Rev Neurobiol 8:25–44
3. Tannenbaum GS, Epelbaum J (1999) Somatostatin In: Kostyo JL, Goodman HM (eds) Handbook of physiology – the endocrine system, vol. V: Hormonal control of growth. Oxford University Press, New York, pp 221–265
4. Krantic S, Quirion R, Uhl G (1992) Somatostatin receptors In: Björklund A, Hökfelt T, Kuhar MJ (eds) Handbook of chemical neuroanatomy, vol. 11: neuropeptide receptors in the CNS. Elsevier, Amsterdam, pp 321–346
5. Patel YC (1999) Somatostatin and its receptor family. Front Neuroendocrinol 20:157–198
6. Csaba Z, Dournaud P (2001) Cellular biology of somatostatin receptors. Neuropeptides 35:1–23
7. Olias G, Viollet C, Kusserow H, Epelbaum J, Meyerhof W (2004) Regulation and function of somatostatin receptors. J Neurochem 89:1057–1091
8. Breder CD, Yamada Y, Yasuda K, Seino S, Saper CB, Bell GI (1992) Differential expression of somatostatin receptor subtypes in brain. J Neurosci 12:3920–3934

9. Kong H, DePaoli AM, Breder CD, Yasuda K, Bell GI, Reisine T (1994) Differential expression of messenger RNAs for somatostatin receptor subtypes SSTR1, SSTR2 and SSTR3 in adult rat brain: analysis by RNA blotting and in situ hybridization histochemistry. Neuroscience 59:175–184
10. Pérez J, Rigo M, Kaupmann K, Bruns C, Yasuda K, Bell GI, Lübbert H, Hoyer D (1994) Localization of somatostatin (SRIF) SSTR−1, SSTR−2 and SSTR−3 receptor mRNA in rat brain by in situ hybridization. Naunyn Schmiedebergs Arch Pharmacol 349:145–160
11. Señaris RM, Humphrey PP, Emson PC (1994) Distribution of somatostatin receptors 1, 2 and 3 mRNA in rat brain and pituitary. Eur J Neurosci 6:1883–1896
12. Raulf F, Pérez J, Hoyer D, Bruns C (1994) Differential expression of five somatostatin receptor subtypes, SSTR1–5, in the CNS and peripheral tissue. Digestion 55 Suppl 3:46–53
13. Beaudet A, Greenspun D, Raelson J, Tannenbaum GS (1995) Patterns of expression of SSTR1 and SSTR2 somatostatin receptor subtypes in the hypothalamus of the adult rat: relationship to neuroendocrine function. Neuroscience 65:551–561
14. Tannenbaum GS, Zhang WH, Lapointe M, Zeitler P, Beaudet A (1998) Growth hormone-releasing hormone neurons in the arcuate nucleus express both Sst1 and Sst2 somatostatin receptor genes. Endocrinology 139:1450–1453
15. Guo F, Beaudet A, Tannenbaum GS (1996) The effect of hypophysectomy and growth hormone replacement on sst1 and sst2 somatostatin receptor subtype messenger ribonucleic acids in the arcuate nucleus. Endocrinology 137:3928–3935
16. Zheng H, Bailey A, Jiang MH, Honda K, Chen HY, Trumbauer ME, Van der Ploeg LH, Schaeffer JM, Leng G, Smith RG (1997) Somatostatin receptor subtype 2 knockout mice are refractory to growth hormone-negative feedback on arcuate neurons. Mol Endocrinol 11:1709–1717
17. Zhang WH, Beaudet A, Tannenbaum GS (1999) Sexually dimorphic expression of sst1 and sst2 somatostatin receptor subtypes in the arcuate nucleus and anterior pituitary of adult rats. J Neuroendocrinol 11:129–136
18. Lanneau C, Bluet-Pajot MT, Zizzari P, Csaba Z, Dournaud P, Helboe L, Hoyer D, Pellegrini E, Tannenbaum GS, Epelbaum J, Gardette R (2000) Involvement of the Sst1 somatostatin receptor subtype in the intrahypothalamic neuronal network regulating growth hormone secretion: an in vitro and in vivo antisense study. Endocrinology 141:967–979
19. Dournaud P, Gu YZ, Schonbrunn A, Mazella J, Tannenbaum GS, Beaudet A (1996) Localization of the somatostatin receptor SST2A in rat brain using a specific anti-peptide antibody. J Neurosci 16:4468–4478
20. Schindler M, Sellers LA, Humphrey PP, Emson PC (1997) Immunohistochemical localization of the somatostatin SST2(A) receptor in the rat brain and spinal cord. Neuroscience 76:225–240
21. Schindler M, Humphrey PP, Lohrke S, Friauf E (1999) Immunohistochemical localization of the somatostatin sst2(b) receptor splice variant in the rat central nervous system. Neuroscience 90:859–874
22. Helboe L, Stidsen CE, Møller M (1998) Immunohistochemical and cytochemical localization of the somatostatin receptor subtype sst1 in the somatostatinergic parvocellular neuronal system of the rat hypothalamus. J Neurosci 18:4938–4945
23. Hervieu G, Emson PC (1998) The localization of somatostatin receptor 1 (sst1) immunoreactivity in the rat brain using an N-terminal specific antibody. Neuroscience 85:1263–1284
24. Schulz S, Schreff M, Schmidt H, Händel M, Przewlocki R, Höllt V (1998) Immunocytochemical localization of somatostatin receptor sst2A in the rat spinal cord and dorsal root ganglia. Eur J Neurosci 10:3700–3708
25. Händel M, Schulz S, Stanarius A, Schreff M, Erdtmann-Vourliotis M, Schmidt H, Wolf G, Höllt V (1999) Selective targeting of somatostatin receptor 3 to neuronal cilia. Neuroscience 89:909–926
26. Stroh T, Kreienkamp HJ, Beaudet A (1999) Immunohistochemical distribution of the somatostatin receptor subtype 5 in the adult rat brain: predominant expression in the basal forebrain. J Comp Neurol 412:69–82
27. Schreff M, Schulz S, Händel M, Keilhoff G, Braun H, Pereira G, Klutzny M, Schmidt H, Wolf G, Höllt V (2000) Distribution, targeting, and internalization of the sst4 somatostatin receptor in rat brain. J Neurosci 20:3785–3797
28. Selmer IS, Schindler M, Humphrey PP, Emson PC (2000) Immunohistochemical localization of the somatostatin sst(4) receptor in rat brain. Neuroscience 98:523–533
29. Meyerhof W, Paust HJ, Schönrock C, Richter D (1991) Cloning of a cDNA encoding a novel putative G-protein-coupled receptor expressed in specific rat brain regions. DNA Cell Biol 10:689–694
30. Yamada Y, Post SR, Wang K, Tager HS, Bell GI, Seino S (1992) Cloning and functional characterization of a family of human and mouse somatostatin receptors expressed in brain, gastrointestinal tract, and kidney. Proc Natl Acad Sci USA 89:251–255
31. Innamorati G, Le Gouill C, Balamotis M, Birnbaumer M (2001) The long and the short cycle. Alternative intracellular routes for trafficking of G-protein-coupled receptors. J Biol Chem 276:13096–13103
32. Sarret P, Perron A, Stroh T, Beaudet A (2003) Immunohistochemical distribution of NTS2 neurotensin receptors in the rat central nervous system. J Comp Neurol 461:520–538
33. Dournaud P, Boudin H, Schonbrunn A, Tannenbaum GS, Beaudet A (1998) Interrelationships between somatostatin sst2A receptors and somatostatin-containing axons in rat brain: evidence for regulation of cell surface receptors by endogenous somatostatin. J Neurosci 18:1056–1071
34. Boudin H, Sarret P, Mazella J, Schonbrunn A, Beaudet A (2000) Somatostatin-induced regulation of SST(2A) receptor expression and cell surface availability in central neurons: role of receptor internalization. J Neurosci 20:5932–5939
35. Sarret P, Krzywkowski P, Segal L, Nielsen MS, Petersen CM, Mazella J, Stroh T, Beaudet A (2003) Distribution of NTS3 receptor/sortilin mRNA and protein in the rat central nervous system. J Comp Neurol 461:483–505
36. Gu YZ, Brown PJ, Loose-Mitchell DS, Stork PJ, Schonbrunn A (1995) Development and use of a receptor antibody to characterize the interaction between somatostatin receptor subtype 1 and G proteins. Mol Pharmacol 48:1004–1014
37. Helboe L, Møller M, Nørregaard L, Schiødt M, Stidsen CE (1997) Development of selective antibodies against the human somatostatin receptor subtypes sst1–sst5. Brain Res Mol Brain Res 49:82–88
38. Roosterman D, Roth A, Kreienkamp HJ, Richter D, Meyerhof W (1997) Distinct agonist-mediated endocytosis of cloned rat somatostatin receptor subtypes expressed in insulinoma cells. J Neuroendocrinol 9:741–751
39. Johansson O, Hökfelt T, Elde RP (1984) Immunohistochemical distribution of somatostatin-like immunoreactivity in the central nervous system of the adult rat. Neuroscience 13:265–339
40. Vincent SR, McIntosh CH, Buchan AM, Brown JC (1985) Central somatostatin systems revealed with monoclonal antibodies. J Comp Neurol 238:169–186
41. Bertherat J, Bluet-Pajot MT, Epelbaum J (1995) Neuroendocrine regulation of growth hormone. Eur J Endocrinol 132:12–24
42. Csaba Z, Bernard V, Helboe L, Bluet-Pajot MT, Bloch B, Epelbaum J, Dournaud P (2001) In vivo internalization of the somatostatin sst2A receptor in rat brain: evidence for translocation of cell-surface receptors into the endosomal recycling pathway. Mol Cell Neurosci 17:646–661

43. Wang H, Gracy KN, Pickel VM (1999) Mu-opioid and NMDA-type glutamate receptors are often colocalized in spiny neurons within patches of the caudate-putamen nucleus. J Comp Neurol 412:132–146
44. Luján R, Nusser Z, Roberts JD, Shigemoto R, Somogyi P (1996) Perisynaptic location of metabotropic glutamate receptors mGluR1 and mGluR5 on dendrites and dendritic spines in the rat hippocampus. Eur J Neurosci 8:1488–1500
45. Luján R, Roberts JD, Shigemoto R, Ohishi H, Somogyi P (1997) Differential plasma membrane distribution of metabotropic glutamate receptors mGluR1 alpha, mGluR2 and mGluR5, relative to neurotransmitter release sites. J Chem Neuroanat 13:219–241
46. Riedel G, Wetzel W, Reymann KG (1996) Comparing the role of metabotropic glutamate receptors in long-term potentiation and in learning and memory. Prog Neuropsychopharmacol Biol Psychiatry 20:761–789